ARTICLES

In situ measurements of the physical characteristics of Titan's environment

M. Fulchignoni[1,2], F. Ferri[3], F. Angrilli[3], A. J. Ball[4], A. Bar-Nun[5], M. A. Barucci[1], C. Bettanini[3], G. Bianchini[3], W. Borucki[6], G. Colombatti[3], M. Coradini[7], A. Coustenis[1], S. Debei[3], P. Falkner[8], G. Fanti[3], E. Flamini[9], V. Gaborit[1], R. Grard[8], M. Hamelin[10,11], A. M. Harri[12], B. Hathi[4], I. Jernej[13], M. R. Leese[4], A. Lehto[12], P. F. Lion Stoppato[3], J. J. López-Moreno[14], T. Mäkinen[12], J. A. M. McDonnell[4], C. P. McKay[6], G. Molina-Cuberos[15], F. M. Neubauer[16], V. Pirronello[17], R. Rodrigo[14], B. Saggin[18], K. Schwingenschuh[13], A. Seiff‡, F. Simões[10], H. Svedhem[8], T. Tokano[16], M. C. Towner[4], R. Trautner[8], P. Withers[4,19] & J. C. Zarnecki[4]

On the basis of previous ground-based and fly-by information, we knew that Titan's atmosphere was mainly nitrogen, with some methane, but its temperature and pressure profiles were poorly constrained because of uncertainties in the detailed composition. The extent of atmospheric electricity ('lightning') was also hitherto unknown. Here we report the temperature and density profiles, as determined by the Huygens Atmospheric Structure Instrument (HASI), from an altitude of 1,400 km down to the surface. In the upper part of the atmosphere, the temperature and density were both higher than expected. There is a lower ionospheric layer between 140 km and 40 km, with electrical conductivity peaking near 60 km. We may also have seen the signature of lightning. At the surface, the temperature was 93.65 ± 0.25 K, and the pressure was 1,467 ± 1 hPa.

Earlier Voyager fly-bys of Titan and telescopic observations indicated that Titan's atmosphere is composed of N_2 with small amounts of CH_4. The surface pressure was determined to be approximately 1,400 hPa, with a surface temperature of about 95 K decreasing to a temperature minimum of about 70 K at 40 km altitude before increasing again to about 170 K in the stratosphere[1–3]. The atmospheric structure at high elevations (1,000–1,500 km) was inferred from the solar occultation measurements by the Voyager ultraviolet spectrometer (UVS)[4]. The middle atmosphere (200–600 km) was not well determined, although telescopic observations indicated a complex vertical structure[5–10] and models have been used to predict the atmospheric structure in this region[11–13]. Very little was known about the surface of Titan because it is hidden by a thick haze and is almost undetectable, except by radar sounding[14] and a few infrared windows that have been observed from telescopes[15,16]. Initial speculation was that the surface was covered by a deep hydrocarbon ocean, but infrared and radar measurements showed definite albedo contrasts—possibly consistent with lakes, but not with a global ocean. Recently, measurements by the Cassini orbiter in the near-infrared and at radar frequencies provided new results on the nature of the surface of the satellite[17–19].

Earlier observations showed that the surface pressure on Titan was comparable to that on the Earth, and that CH_4 formed a plausible counterpart to terrestrial H_2O for cloud and rain formation. There was also speculation on the possibility of lightning occurring in Titan's atmosphere[20–22] which could affect the chemical composition of the atmosphere.

In this Article, we report results from the HASI instrument on the Huygens probe[23]. By monitoring the probe deceleration, the HASI instrument directly determined the density of the upper atmosphere and derived the temperature from the density scale height. In the lower atmosphere and on the surface of Titan, the HASI instrument directly measured the pressure and temperature. During the probe descent, electrical activity was monitored to search for evidence of lightning activity. A search for acoustic signals produced by any thunder or other shock waves was also conducted. A comprehensive description of the HASI instrument can be found in ref. 24.

In the upper atmosphere, the density profile is used to infer the temperature profile. Above 500 km, the temperature structure shows strong wave-like variations of 10–20 K about a mean of about 170 K. Below 500 km, the temperature increases to a relative maximum of 186 K and then reaches an absolute minimum of 70 K at 44 km. Below about 200 km, the temperature and pressure profile measured by HASI agrees with the results of the Voyager radio occultation data[2]. The surface temperature is determined to be 93.65 ± 0.25 K, and the surface pressure is 1,467 ± 1 hPa. The values are within the range allowed by the uncertainties in the Voyager data[13] owing to previous uncertainties in the mixing ratio of CH_4 and argon. Electrical conductivity measurements indicate the presence of charged particle

[1]LESIA, Observatoire de Paris, 5 Place Janssen, 92195 Meudon, France. [2]Université Denis Diderot – Paris 7, UFR de Physique, 2 Place Jussieu, 75006 Paris, France. [3]CISAS "G. Colombo", Università di Padova, Via Venezia 15, 35131 Padova, Italy. [4]PSSRI, The Open University, Walton Hall, Milton Keynes MK7 6AA, UK. [5]Department of Geophysics and Planetary Sciences, University of Tel Aviv, 69978 Tel Aviv, Israel. [6]NASA/AMES Research Center, MS 244-30, Moffett Field, California 94035, USA. [7]ESA Headquarters, Science Directorate, 8-10 rue Mario-Nikis, 75015 Paris, France. [8]ESA-ESTEC, European Space Agency, Keplerlaan 1, 2200 AG Noordwijk, The Netherlands. [9]Agenzia Spaziale Italiana, Viale Liegi 26, 00198 Roma, Italy. [10]CETP-IPSL, 4 Avenue de Neptune, 94107 Saint Maur, France. [11]LPCE-CNRS, 3A, Avenue de la Recherche Scientifique, 45071 Orléans cedex 2, France. [12]Finnish Meteorological Institute (FMI), Vuorikatu 15 A 00100 Helsinki, Finland. [13]Space Research Institute, Austrian Academy of Sciences (IWF), Schmiedlstrasse 6, 8042 Graz, Austria. [14]Instituto de Astrofisica de Andalucia (IAA-CSIC), PO Box 3004, 18080 Granada, Spain. [15]Applied Electromagnetic Group, Department of Physics, University of Murcia, Murcia 30100, Spain. [16]Institut für Geophysik und Meteorologie, Universität zu Köln, Albertus-Magnus-Platz, 50923 Köln, Germany. [17]DMFCI, Università di Catania, Viale A. Doria 6, 95125 Catania, Italy. [18]Politecnico di Milano, Dipartimento di Meccanica, Piazza Leonardo da Vinci 32, 20133 Milano, Italy. [19]Center for Space Physics, Boston University, 725 Commonwealth Avenue, Boston, Massachusetts 02215, USA.
‡Deceased.

species in an ionized layer, presumably induced by cosmic rays, and the detection of some electrical discharges.

Atmosphere

We inferred the atmospheric structure of Titan on the basis of measurements taken during entry phase and while the probe was descending under the parachutes. The atmosphere was first detected at an altitude of ~1,500 km, when it exceeded the sensitivity threshold of the accelerometer[25]. Broadly speaking, the temperature and density of the upper atmosphere exceeded predictions. Titan's atmosphere is apparently highly stratified. The density of the upper atmosphere was derived from the probe deceleration due to aerodynamic drag force, following a method[24,25] previously used for other planetary atmospheres such as Venus, Mars and Jupiter. The velocity as a function of time was determined by integrating the measured probe deceleration. Altitude was determined by integrating the vertical component of the velocity using the state vector of the probe provided by the Cassini navigation team. The entry altitude has a 1σ uncertainty of about 30 km; we adjusted the nominal entry altitude within this standard deviation to ensure consistency between the entry phase and descent phase measurements[26].

The derived density profile is shown in Fig. 1, with a comparison of the engineering model[13] obtained from the reanalysis[2–4,11,12] of Voyager data (radio occultations, infrared interferometry (IRIS) and UVS spectrometers). In the upper part of the atmosphere down to an altitude of about 500 km, the HASI measurements show density values systematically higher than those expected. Pressures were obtained from the density profile under the assumption of hydrostatic equilibrium and the knowledge of planetary gravity (1.354 m s^{-2} at surface level), mass (1.35×10^{23} kg) and radius (2,575 km). Temperatures were derived from the pressures, the inferred densities and the equation of state of a perfect gas using the atmospheric mean molecular weight, as a function of altitude given by the engineering model. The pressure versus temperature profile of Titan's atmosphere is shown in Fig. 2. The thermosphere is characterized by the presence of temperature variations due to inversion layers or other dynamic phenomena (such as gravity waves and gravitational tides) between 500 km and 1,020 km.

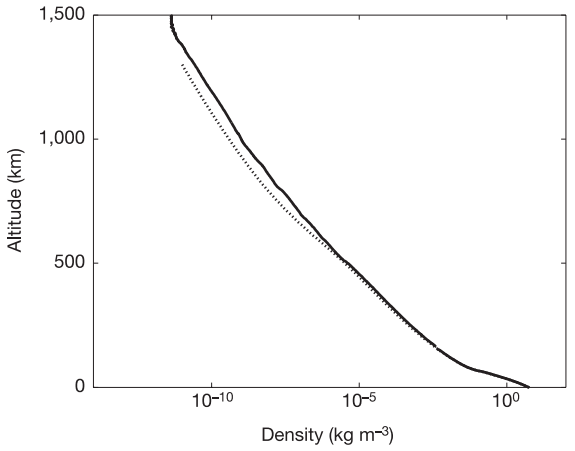

Figure 1 | The atmospheric density profile of Titan as measured by HASI. The density profile as derived from HASI measurements (solid line) is shown in comparison with the engineering model of Titan's atmosphere[13] derived from Voyager 1 data[2–4,11,12] (dashed line). Density in the upper part of the atmosphere is derived from the ACC accelerometer data. The threshold density was 5×10^{-12} kg m^{-3}. The uncertainty on the density determination[25] is of the order of 10%, mainly due to the uncertainty on the aerodynamic drag coefficient and on the probe velocity. Density values relevant to the lower atmosphere, below 160 km, have been inferred from HASI direct measurements of pressure and temperature with the assumption of hydrostatic equilibrium and real gas law[29].

Temperatures in this region are generally higher than those predicted by the engineering model, with a minimum value of 152 K at an altitude of ~490 km (2×10^{-3} hPa, which could mark the mesopause) and then increase down to the stratopause (~186 K at 250 km, 0.3 hPa). In the region between the lower part of the mesosphere and the upper part of the stratosphere, the temperatures are 5–10 K higher than those predicted by the model[12].

The temperature gradient profile, shown in Fig. 3, exhibits in general a cut-off at the dry adiabatic lapse rate, implying that fluctuations lead to marginally convective instabilities. The inversion layers in the upper atmosphere are clearly visible, with strong peaks towards positive values. The peak at 510 km corresponds to the inversion layer already observed from the ground on 14 November 2003 when Titan occulted two bright Tycho stars[10]. These lines of evidence all indicate that Titan's atmosphere is highly stratified.

After the parachute deployment and heatshield separation, the temperature sensors[27] and pressure sensors[28] were directly exposed to Titan's environment during the entire descent under parachute. The altitude and velocity are derived from these measurements, the hypothesis of hydrostatic equilibrium, and the equation of state for a real gas[29], given the atmospheric mean molecular weight measured by the Gas Chromatograph-Mass Spectrometer (GCMS)[30]. The measured pressure and temperature profiles shown in Figs 4 and 5 connect well with the profiles derived during the entry phase. From the surface up to about 150 km altitude, the HASI temperatures are in very good agreement (within 1–2 K) with the temperature measurements obtained by the Voyager 1 radio occultation assuming a pure nitrogen atmosphere[2].

The temperature minimum of 70.43 ± 0.25 K is reached at the tropopause (~44 km, 115 hPa). Figure 6 shows the temperature lapse rate in the low atmosphere. A number of inversion layers in the lower stratosphere and the strong increase in temperature with altitude between 80 km and 60 km are visible. Below 200 km, the fine

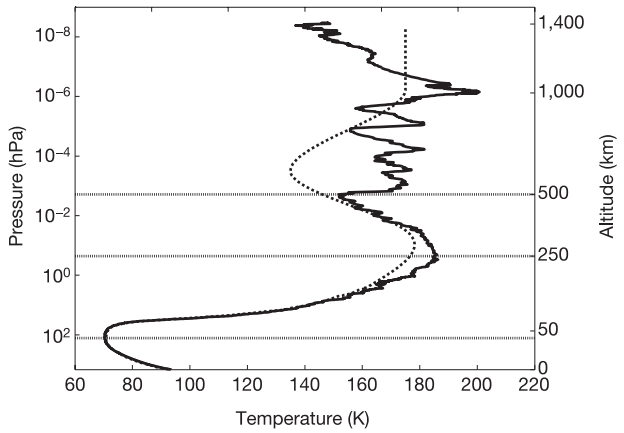

Figure 2 | The atmospheric temperature profile. The temperature profile as measured by HASI (solid line) is shown compared to Titan's atmospheric engineering model[13] (dashed line). In the upper atmosphere (above 160 km), temperature and pressure have been derived from the density using the ideal gas equation; below 160 km, temperature data are direct measurements collected by the TEM sensor. The temperature profile in the upper atmosphere (thermosphere) is characterized by several temperature variations due to inversion layers and other dynamic phenomena (for example, gravity waves and tides). Temperatures in this region are higher than those predicted by the model. The virtual absence of a mesosphere (in contrast with the theoretical models' predictions[11,12]) and the wave-like nature of the temperature profile suggest that the region in Titan's atmosphere above 250 km may not be dominated by radiative processes and may be strongly influenced by wave activity. Thus the structure that we observe may vary with time. The horizontal lines mark the mesopause (152 K at 490 km), the stratopause (186 K at 250 km) and the tropopause (70.43 K at 44 km).

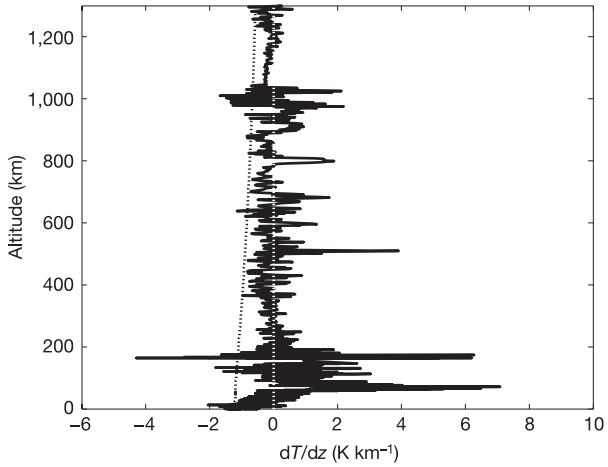

Figure 3 | The temperature lapse rate. The temperature gradient dT/dz was computed from the HASI temperature ($T(z)$) profile, and the altitude (z) was derived from the Huygens trajectory reconstruction[26]. The spatial resolution of the HASI measurements is of the order of 20 km from the top of the atmosphere down to the 400-km altitude level, decreasing down to 1 km at the 160-km level[24]. The profile shows in general a cut-off at the dry adiabatic lapse rate (dotted line), implying that fluctuations may lead to convective instabilities. The line at zero temperature variation is shown in white against the black curve. Six inversion layers in the upper atmosphere (at about 510, 600, 680, 800, 980 and 1,020 km) could be detected by strong peaks towards positive values. The strong lower inversion layer (4 K km^{-1} at ~510 km) corresponds to the feature already observed from the ground during Titan's stellar occultations[10]. The strong peaks between the 160- and 110-km levels correspond to the parachute deployment sequence.

structure seen in Fig. 5 provides evidence for a regime of gravity waves similar to those observed in the Voyager radio occultation data[31,32]. Turbulence due to shear instability (Kelvin–Helmholtz instability) is expected wherever the vertical shear of the wind speed is large. The wind shear measured by the Doppler Wind Experiment[33] is sufficiently large that the features present between 50 and 150 km are likely to be related to turbulence.

The vertical resolution of the temperature measurement was sufficient to resolve the instantaneous structure of the planetary boundary layer. On the basis of the nearly constant values of the potential temperature, the convective planetary boundary layer had a thickness of about 300 m at the place and time of landing.

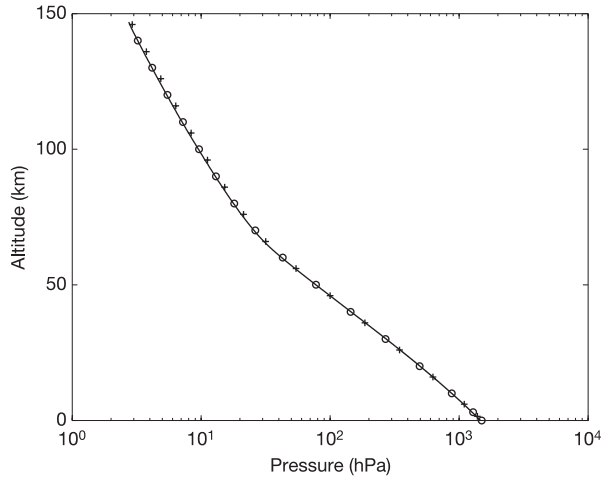

Figure 4 | Pressure profile of the lower atmosphere as measured by the Pressure Profile Instrument (PPI)[28]. Measurements (solid line) corrected for dynamic effects are shown together with values obtained by Voyager 1 radio occultation[2] (ingress, circles; egress, crosses). HASI pressure values are determined with an uncertainty of 1% along the entire descent.

Atmospheric electricity

Models of Titan's ionosphere predicted that galactic cosmic rays would produce an ionospheric layer with a maximum concentration of electrons between 70 and 90 km altitude[34–37]. The Permittivity, Wave and Altimetry package[20] (PWA) measured the electrical state of the atmosphere below 140 km. We found that the electrical conductivity peaks at ~60 km. We might have seen evidence for lightning.

Observations of the electron and ion conductivities were made with two different techniques: relaxation and mutual impedance probes. The results of the relaxation probes (shown in Fig. 7a, b) indicate peaks in the electron/negative-ion conductivities at 60 km. Figure 7c shows that the altitude of the maximum in the conductivity (60 km) is confirmed by the mutual impedance probe measurements. This instrument gives the impedance of the medium at 45 Hz and yields a phase shift, which is sensitive to the presence of electrons only. The quadrupolar probe also records the spectrum of the electric signal induced in the probe environment by the 45 Hz stimulus, in the bandwidth 0–9.22 kHz (Fig. 8a, active mode).

The electric field due to natural wave emissions was investigated during the descent, using the receiving dipole of the mutual impedance probe in two frequency ranges, 0–11.5 kHz and 0–100 Hz (Fig. 8b, c, passive mode). This provided a unique opportunity to investigate *in situ* lightning and related phenomena (for example, corona discharges) on Titan[21] that would produce electromagnetic waves[38], excite global and local resonance phenomena in the surface–ionospheric cavity[39,40] and could drive a global electric circuit[22]. Several impulsive events have been observed during the descent, for example at 2,800 s. The narrow-band wave emission seen near 36 Hz is reminiscent of a possible resonance generated by lightning activity in the spherical waveguide formed by the surface of Titan and the inner boundary of its ionosphere, but should be interpreted with caution. A comparison of the records presented in Fig. 8a and b shows that the first spectrogram (active mode) not only displays the

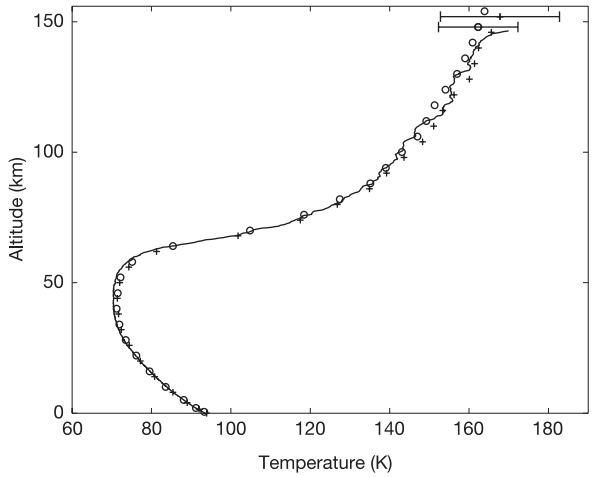

Figure 5 | Temperature profile of the lower atmosphere as measured by the temperature sensors, TEM[27] (expanded from Fig. 2). Temperature uncertainty is ±0.25 K in the range from 60 to 110 K, and ±1 K above 110 K. The temperature minimum of 70.43 K is reached at the tropopause (about 44 km; 115 ± 1 hPa). HASI temperatures are in very good agreement (within the error bars) with data obtained by Voyager radio occultation[2] (ingress, circles; egress, crosses) assuming a pure nitrogen atmosphere. The error bars for Voyager data are reported: ±15 K (egress) ±10 K (ingress) near the 200-km level, ±0.5 K at the tropopause. At the tropopause, HASI measured temperature values ~1 K colder than Voyager[2], but reanalysis of these data[3] suggested a similar temperature value (70.5 K) assuming a stratospheric composition of 98.5% N_2 plus 1.5% CH_4.

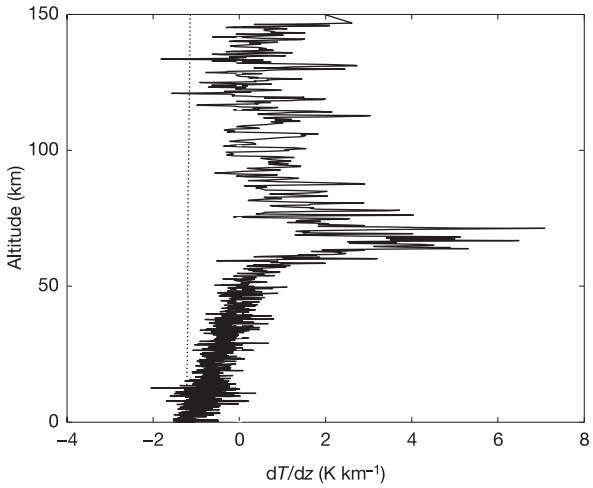

Figure 6 | The temperature lapse rate for the low atmosphere (expanded from Fig. 3). A number of inversion layers in the lower stratosphere and the strong temperature increase with altitude between 80 and 60 km are visible. Features present between 50 and 150 km could be related to turbulence due to Kelvin–Helmholtz instability induced by the large vertical shear of the wind speed, measured by the Doppler Wind Experiment[33]. The temperature gradient in this part of the atmosphere has been derived from direct temperature measurements with vertical spatial resolution of the order of 200–150 m above 60-km altitude, and decreasing from 70 m down to 11 m until the last kilometre.

signals seen in the second spectrogram (passive mode), but also includes a broadband emission in the altitude range 110–80 km, and to lesser extent at altitudes lower than 25 km. It is believed that the energy injected in the medium at 45 Hz is partly dissipated in nonlinear effects, which seems to strengthen the evidence for the presence of free charges in the upper atmosphere.

Surface

Before the probe landed, the nature of the surface was unknown. From the abundance of methane in its atmosphere, there was speculation that Titan might be covered by a methane ocean[41], but recent observations[14] have restricted the fraction of the surface covered with liquid to be just a few per cent. The probe touched down on a solid surface, which has properties something like wet sand[42]. The instruments continued to monitor the meteorological conditions for almost half an hour after impact.

The nature of Titan's surface at the landing site was investigated by spectral analysis of the Huygens radar return signal, the recording of the impact signature, *in situ* measurements of the ground electrical properties, and the surface environmental conditions.

The piezoresistive accelerometers of HASI recorded the impact instant at $T_0 + 2\text{h}\,27\text{min}\,49.840\,\text{s}$ (where T_0 is the time of the parachute deployment device firing and corresponds to the beginning of the descent phase), when the event exceeded the threshold of $\sim 40\,\text{m}\,\text{s}^{-2}$. A complete trace of the impact in the three orthogonal reference axes is shown in Fig. 9. The initial small peak in the X accelerometer data preceding the impact of the main probe may be related to a touch down on uneven topography, or the possible initial contact of a portion of the probe foredome, given the likely probe tilt at landing[42]. A sharp drop in acceleration is seen briefly in all three sensors at 8,869.86 s. The peak probe deceleration measured is $141\,\text{m}\,\text{s}^{-2}$, in reasonable agreement with the value measured by the accelerometer of the Science Surface Package (SSP)[42]. Over the length of the full data set, two possible events are seen in all three axes, at impact ($\sim$8,869.86 s) and $\sim$3 s later at $\sim$8,872.2 s. These correspond respectively to the initial impact event, and then to some short-term settling that may be surface related, or probe related (parachute system dynamics or structural relaxation of foredome). Further

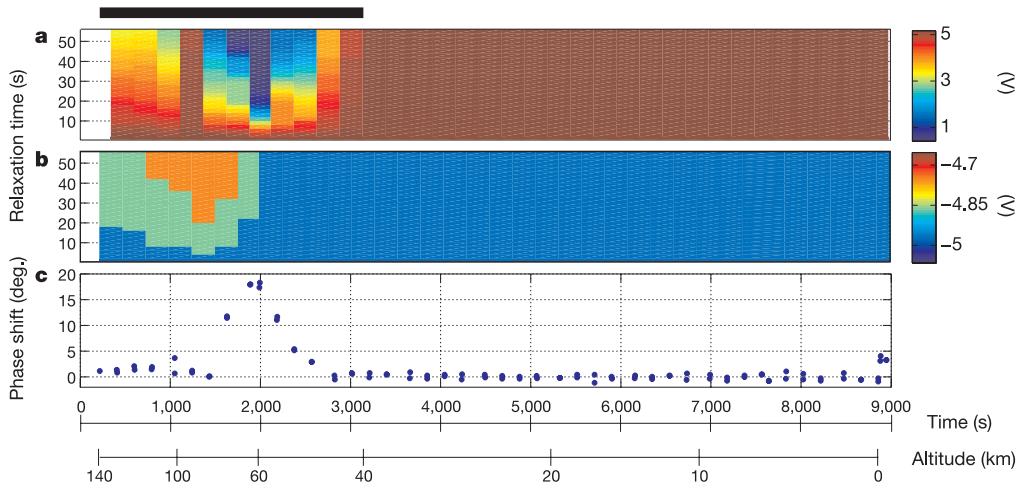

Figure 7 | A synopsis of PWA data: the signature of the ionosphere. The approximate extent of the ionized layer due to the interaction of cosmic rays with the atmosphere is indicated by a thick black line along the top axis. **a**, **b**, Relaxation carpets for $\Phi_o = +5$ V and -5 V, respectively. The relaxation probe, initially biased at a potential Φ_o with respect to the vehicle body, subsequently returns to its equilibrium potential, Φ_∞, with a time constant that yields the d.c. conductivity of the charges with polarity opposite to that of $\Phi_o - \Phi_\infty$. The measurements taken during each relaxation cycle form a string of pixels aligned with the ordinate axis; voltages are given by the colour scales shown on the right-hand side. The electrode potential is measured every 20 ms during the first second, then every 2 s for the reminder of each 1 min cycle. These panels give a visual impression of the speed at which the potential of a conductive body (colour coded) returns from ± 5 V to zero ('relaxes'), owing to the collection of ambient charges with opposite polarities. In the lower altitude range, for example, the colour of the carpet is uniform (brown for $+5$ V and blue for -5 V), which shows that the ambient charge densities are low. Above 40 km, on the contrary, the distinctive carpet patterns tell us that the probe voltage is strongly affected by the ionized environment. **c**, Mutual impedance phase shift, $\Delta\phi = \phi_o - \phi$ (non-calibrated). The a.c. conductivity is measured with a quadrupolar array. A current I with frequency 45 Hz and amplitude $\sim 10^{-10}$ A is injected between two transmitting electrodes, and the voltage V induced between two receiving electrodes 2 m apart is measured. If the phase of V/I at 45 Hz is ϕ_o in a vacuum and ϕ in a collisional medium, then the conductivity of the medium is proportional to $\tan(\phi_o - \phi)$.

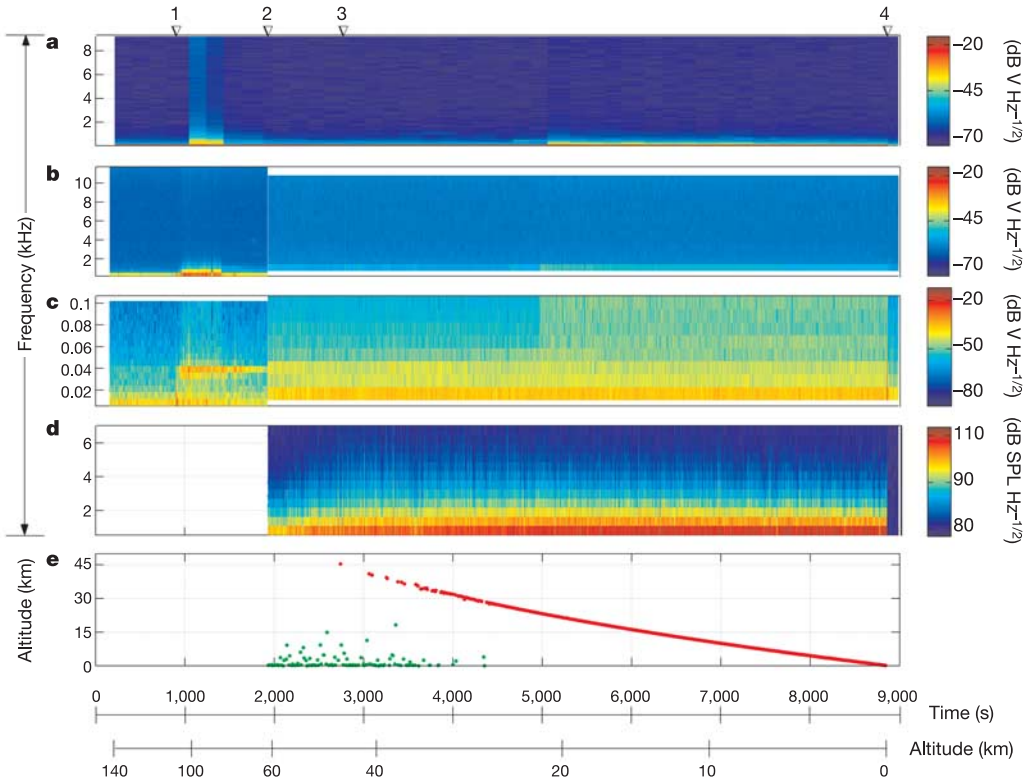

Figure 8 | A synopsis of PWA data: electric field, acoustic pressure and radar measurements. **a**, Dynamic spectrum of the voltage *V* measured between two electrodes 2 m apart, in the bandwidth 0–9.22 kHz, when a current stimulus *I* is injected between two transmitting electrodes. The spectrum of the signal provides information about its energy distribution as a function of frequency, at a given time. Successive spectra are represented by adjacent strings of pixels aligned with the ordinate axis, where spectral amplitude is coded in colour according to the logarithmic scale shown on the right-hand side. **b**, Dynamic spectrum of the voltage *V* measured with two electrodes 2 m apart, in the bandwidth 0–11.5 kHz, without current stimulus. **c**, Same as **b**, but in 0–100 Hz bandwidth. **d**, Dynamic spectrum of acoustic differential pressure in the bandwidth 0–6.7 kHz. A sound pressure level (SPL) of 0 dB corresponds to 20 μPa. The variability of the acoustic noise is caused by changes in the atmospheric density and wind velocity[50]. **e**, The altitude represented by the red dots is measured whenever the Radar Altimeter (RA) is locked on the surface; permanent lock is maintained from 34 km down to 150 m. At higher altitudes, the green dots indicate the distances at which the signal is returned by the atmosphere. Several events are identified with triangles along the top axis: (1) stabilizer parachute opening, (2) mode change, (3) impulsive event in **b**, (4) surface touch down. Discontinuities in time or frequency are artefacts due to mode change.

modelling of the probe structure behaviour is required to quantify these effects. Additionally, the area of stable data points immediately following the initial impact (8,870.1–8,870.3 s) may be due to a small bounce of the probe or to some structure vibrations. Integration of Y and Z axes after further processing, in combination with other sensors, will indicate any possible probe lateral movement. The integration of the accelerometer data gives a probe impact velocity of 4.33 m s^{-1}, in reasonable agreement with the values obtained by SSP[42] and from the velocity profile during the last kilometre of the descent as derived from pressure measurements. For the final rest position of the probe, the X servo accelerometer gives an estimate of the probe tilt of about 11°, in good agreement with SSP tilt sensors.

At the surface, the HASI temperature and pressure sensors monitored the meteorological conditions for almost half an hour after the impact, measuring a temperature of 93.65 ± 0.25 K and a pressure of 1,467 ± 1 hPa. The complex permittivity of the surface material is measured after impact with the PWA mutual impedance probe[43], at five frequencies. As a first estimation, the mean relative permittivity within the sensor range (radius 1 m, depth 2 m) is of the order of 2, in reasonable agreement with the measurements performed with the radar on board Cassini[19].

In addition to providing altitude (Fig. 8), the Radar Altimeter measures the signal backscattered within the footprint of the beam, whose diameter is 0.14 times the altitude. This signal is strong and smooth with small variations over the ground track, indicating a

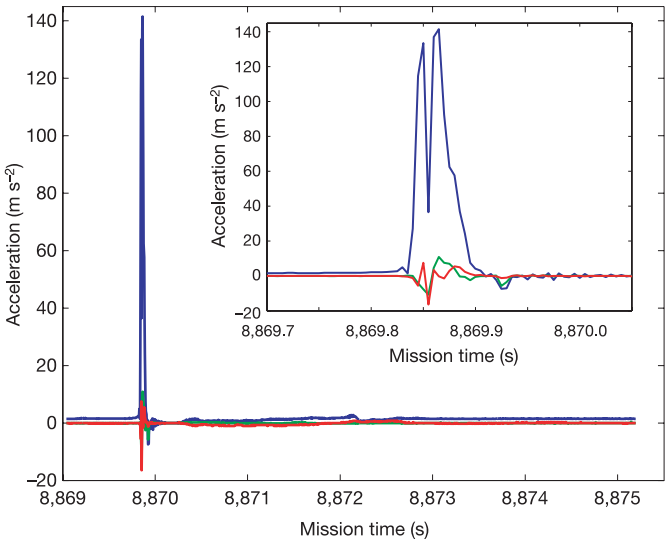

Figure 9 | The HASI signature of the impact trace, at 200 samples per second. The complete impact trace (6 s) is shown; the inset shows a magnified view of the deceleration peak. The X sensor (blue line) is aligned to the probe symmetry axis, corresponding to the descent direction. The Y (green line) and Z (red line) sensors are mounted orthogonal to the Huygens probe symmetry axis.

surface with little relief. The atmosphere was scanned and return signal from droplets was searched for, but no significant signature of rain could be found.

Discussion

Although the HASI data have now provided a great wealth of information on the conditions in the atmosphere and at the surface of Titan, many questions and challenges remain.

Atmospheric structure. The HASI temperature profile in the lower atmosphere was compared to the separate egress and ingress profiles based on the Voyager occultation experiment 25 years earlier. This comparison suggests that the atmosphere of Titan in mid-latitudes is uniform and slowly changing in accordance with model predictions. The open question is the poleward extent of this non-variability, given the latitudinal temperature gradient in the stratosphere inferred from infrared data[44,45]. One interpretation of the south polar clouds is that they are due to heating associated with polar summer warming[46,47]. If this is true, then the temperature profile in the polar summer should be different from the mid-latitude profiles sampled here, and could be revealed by Cassini infrared mapping[45] and radio science[48]. In the middle and upper atmosphere (above 300 km), the prominent wave-like structure reported here requires further modelling to unambiguously identify the causal mechanisms. The observed vertical variation would suggest that large-scale temperature gradient in this region is also time variable. Unfortunately, the necessary observations of the time and spatial evolution of these structures must await future missions.

The atmosphere was scanned by the radar altimeter (before getting in lock), but no significant signature of rain was found. The instrument sensitivity to mass loadings of methane or other hydrocarbon droplets needs to be determined so that an upper limit to droplet mass loadings can be estimated.

Atmospheric electricity. The maximum in the conductivity due to positive ions, 20 km above the peak electron conductivity at 60 km, demands the presence of sufficient aerosols or electrophilic species in order to preserve charge neutrality. The altitude of the maximum conductivity due to electrons lies below that predicted by theoretical models[35–37]. Several pulses similar to terrestrial sferics (natural electromagnetic waves) have been observed during the descent. Large convective clouds were observed near the south pole during the summer season[17] and low-frequency electromagnetic waves could easily propagate from the south pole to the Huygens location. Lightning activity would also be consistent with the observations of waves in the Schumann frequency range.

Nature of the surface. The lack of any rhythmic motion during the half hour of operation on the surface indicated that the probe had landed on a solid surface rather than a liquid, which agrees with the image taken after the landing[49]. The measured relative permittivity (of the order of 2) constrains the soil composition. No evidence for the presence of liquid phase on the surface was returned by the signal of the radar altimeter.

The HASI measurements of the atmospheric structure, electrical state and surface properties provide a unique insight into Titan's characteristics, unequalled in any planetary atmosphere except the Earth's. The many discoveries and puzzles will require synergetic analysis with the Cassini orbiter observations and years of laboratory and modelling efforts to solve.

Received 28 May; accepted 11 October 2005.
Published online 30 November 2005.

1. McKay, C. P., Pollack, J. B. & Courtin, R. The thermal structure of Titan's atmosphere. *Icarus* **80,** 23–53 (1989).
2. Lindal, G. F. *et al.* The atmosphere of Titan—an analysis of the Voyager 1 radio occultation measurements. *Icarus* **53,** 348–363 (1983).
3. Lellouch, E. *et al.* Titan's atmosphere and hypothesized ocean: a reanalysis of the Voyager 1 radio-occultation and IRIS 7.7 μm data. *Icarus* **79,** 328–349 (1989).
4. Vervack, R. J., Sandel, B. R. & Strobel, D. F. New perspectives on Titan's upper atmosphere from a reanalysis of the Voyager 1 UVS solar occultations. *Icarus* **170,** 91–112 (2004).
5. Coustenis, A. *et al.* Titan's atmosphere from ISO mid-infrared spectroscopy. *Icarus* **161,** 383–403 (2003).
6. Hubbard, W. B. *et al.* Results for Titan's atmosphere from its occultation of 28 Sagittarii. *Nature* **343,** 353–355 (1990).
7. Sicardy, B. *et al.* The structure of Titan's stratosphere from the 28 Sgr occultation. *Icarus* **142,** 357–390 (1999).
8. Tracadas, P. W., Hammel, H. B., Thomas-Osip, J. E. & Elliot, J. L. Probing Titan's atmosphere with the 1995 August stellar occultation. *Icarus* **153,** 285–294 (2001).
9. Bouchez, A. H. *et al.* Adaptive optics imaging of a double stellar occultation by Titan. *Bull. Am. Astron. Soc.* **34,** 881 (2002).
10. Sicardy, B. *et al.* The two stellar occultations of November 14, 2003: revealing Titan's stratosphere at sub-km resolution. *Bull. Am. Astron. Soc.* **36,** 1119 (2004).
11. Lellouch, E., Hunten, D., Kockarts, G. & Coustenis, A. Titan's thermosphere profile. *Icarus* **83,** 308–324 (1990).
12. Yelle, R. V. Non-LTE models of Titan's upper atmosphere. *Astrophys. J.* **383,** 380–400 (1991).
13. Yelle, R. V., Strobel, D. F., Lellouch, E. & Gautier, D. *Engineering Models for Titan's Atmosphere* 243–256 (ESA SP-1177, European Space Agency, Noordwijk, 1997).
14. Campbell, D. B., Black, G. J., Carter, L. M. & Ostro, S. J. Radar evidence for liquid surfaces on Titan. *Science* **302,** 431–434 (2003).
15. Coustenis, A. *et al.* Maps of Titan's surface from 1 to 2.5 μm. *Icarus* **177,** 89–105 (2005).
16. Meier, R., Smith, B. A., Owen, T. C. & Terrile, R. J. The surface of Titan from NICMOS observations with the Hubble Space Telescope. *Icarus* **145,** 462–473 (2000).
17. Porco, C. C. *et al.* Imaging of Titan from the Cassini spacecraft. *Nature* **434,** 159–168 (2005).
18. Brown, R. H. *et al.* Cassini Visual and Infrared Mapping Spectrometer (VIMS): Results for the SOI- and near-SOI period of the Cassini orbital tour. *Astron. Astrophys.* (submitted).
19. Elachi, C. *et al.* Cassini radar views the surface of Titan. *Science* **308,** 970–974 (2005).
20. Grard, R. *et al.* An experimental investigation of atmospheric electricity and lightning activity to be performed during the descent of the Huygens probe onto Titan. *J. Atmos. Terr. Phys.* **57,** 575–578 (1995).
21. Desch, S. J., Borucki, W. J., Russell, C. T. & Bar-Nun, A. Progress in planetary lightning. *Rep. Prog. Phys.* **65,** 955–997 (2002).
22. Tokano, T., Molina-Cuberos, G. J., Lammer, H. & Stumptner, W. Modelling of thunderclouds and lightning generation on Titan. *Planet. Space Sci.* **49,** 539–560 (2001).
23. Lebreton, J.-P. & Matson, D. L. The Huygens probe: science, payload and mission overview. *Space Sci. Rev.* **104,** 59–100 (2002).
24. Fulchignoni, M. *et al.* The characterization of Titan's atmospheric physical properties by the Huygens Atmospheric Structure Instrument (HASI). *Space Sci. Rev.* **104,** 395–431 (2002).
25. Zarnecki, J. C. *et al. In-Flight Performances of the Servo Accelerometer and Implication for Results at Titan* 71–76 (ESA SP-544, European Space Agency, Noordwijk, 2004).
26. Lebreton, J. P. *et al.* An overview of the descent and landing of the Huygens probe on Titan. *Nature* doi:10.1038/nature04347 (this issue).
27. Ruffino, G. *et al.* The temperature sensor on the Huygens probe for the Cassini mission: Design, manufacture, calibration and tests of the laboratory prototype. *Planet. Space Sci.* **44–10,** 1149–1162 (1996).
28. Harri, A.-M. *et al.* Scientific objectives and implementation of the Pressure Profile Instrument (PPI/HASI) for the Huygens spacecraft. *Planet. Space Sci.* **46,** 1383–1392 (1998).
29. Mäkinen, T. Processing the HASI measurements. *Adv. Space Res.* **17,** 217–222 (1996).
30. Niemann, H. B. *et al.* The abundances of constituents of Titan's atmosphere from the GCMS instrument on the Huygens probe. *Nature* doi:10.1038/nature04122 (this issue).
31. Hinson, D. P. & Tyler, G. L. Internal gravity waves in Titan's atmosphere observed by Voyager radio occultation. *Icarus* **54,** 337–352 (1983).
32. Friedson, A. J. Gravity waves in Titan's atmosphere. *Icarus* **109,** 40–57 (1994).
33. Bird, M. K. *et al.* The vertical profile of winds on Titan. *Nature* doi:10.1038/nature04060 (this issue).
34. Molina-Cuberos, G. J., López-Moreno, J. J., Rodrigo, R. & Lara, L. M. Chemistry of the galactic cosmic ray induced ionosphere of Titan. *J. Geophys. Res.* **104,** 21997–22024 (1999).
35. Borucki, W. J. *et al.* Predictions of the electrical conductivity and charging of the aerosols in Titan's atmosphere. *Icarus* **72,** 604–622 (1987).
36. Borucki, W. J., Whitten, R. C., Bakes, E. L. O., Barth, E. & Tripathi, S. Predictions of the electrical conductivity and charging of the aerosols in Titan's atmosphere. *Icarus* (in the press).
37. Molina-Cuberos, G. J., López-Moreno, J. J., Rodrigo, R. & Schwingenschuh, K. Capability of the Cassini/Huygens PWA-HASI to measure electrical conductivity in Titan. *Adv. Space Res.* **28,** 1511–1516 (2001).

38. Schwingenschuh, K. *et al.* Propagation of electromagnetic waves in the lower ionosphere of Titan. *Adv. Space Res.* **28,** 1505–1510 (2001).
39. Nickolaenko, A. P., Besser, B. P. & Schwingenschuh, K. Model computations of Schumann resonance on Titan. *Planet. Space Sci.* **51,** 853–862 (2003).
40. Morente, J. A., Molina-Cuberos, G. J., Portí, J. A., Schwingenschuh, K. & Besser, B. P. A study of the propagation of electromagnetic waves in Titan's atmosphere with the TLM numerical method. *Icarus* **162,** 374–384 (2003).
41. Lunine, J. I., Stevenson, D. J. & Yung, Y. L. Ethane ocean on Titan. *Science* **222,** 1229–1230 (1983).
42. Zarnecki, J. C. *et al.* A soft solid surface on Titan as revealed by the Huygens Surface Science Package. *Nature* doi:10.1038/nature04211 (this issue).
43. Hamelin, M. *et al.* Surface and sub-surface electrical measurement of Titan with the PWA-HASI experiment on Huygens. *Adv. Space Res.* **26,** 1697–1704 (2000).
44. Coustenis, A. & Bézard, B. Titan's atmosphere from Voyager infrared observations. IV. Latitudinal variations of temperature and composition. *Icarus* **115,** 126–140 (1995).
45. Flasar, F. M. *et al.* Titan's atmospheric temperatures, winds, and composition. *Science* **308,** 975–978 (2005).
46. Brown, M. E., Bouchez, A. H. & Griffith, C. A. Direct detection of variable tropospheric clouds near Titan's south pole. *Nature* **420,** 7995–7997 (2002).
47. Tokano, T. Meteorological assessment of the surface temperatures on Titan: constraints on the surface type. *Icarus* **173,** 222–242 (2005).
48. Kliore, A. J. *et al.* Cassini Radio Science. *Space Sci. Rev.* **115,** 1–70 (2004).
49. Tomasko, M. G. *et al.* Rain, winds and haze during the Huygens probe's descent to Titan's surface. *Nature* doi:10.1038/nature04126 (this issue).
50. Ksanfomaliti, L. V. *et al.* Acoustic measurements of the wind velocity at the Venera 13 and Venera 14 landing sites. *Sov. Astron. Lett* **8(**4), 227–229 (1982).

Acknowledgements We thank the following people for their contributions to the realization of the HASI experiment: A. Buccheri, R. DeVidi, and M. Cosi of Galileo Avionica, A. Aboudan, S. Bastianello and M. Fabris of CISAS, M. Chabassière of LPCE, V. Brown, J.M. Jeronimo and L.M. Lara of IAA, R. Hofe of IWF, A. Smit, L. Smit and J. Van der Hooke from RSSD-ESTEC, H. Jolly from the UK, R. Pellinen, G. Leppelmeier, T. Siili, P. Salminen from FMI, and at the Aerodynamics Laboratory of Helsinki University of Technology T. Siikonen and B. Fagerström. HASI has been realised and operated by CISAS under a contract with the Italian Space Agency (ASI), with the participation of RSSD, FMI, IAA, IWF, LPCE and PSSRI sponsored by the respective agencies: ESA, TEKES, CSIC, BM:BWK, CNES and PPARC. We also acknowledge the long years of work by some hundreds of people in the development and design of the Huygens probe. The Huygens probe is part of the Cassini-Huygens mission, a joint endeavour of the National Aeronautics and Space Administration (NASA), the European Space Agency (ESA) and the Italian Space Agency (ASI).

Author Information Reprints and permissions information is available at npg.nature.com/reprintsandpermissions. The authors declare no competing financial interests. Correspondence and requests for materials should be addressed to F.F. (francesca.ferri@unipd.it).